

Solution of Flow and Heat Transfer of an Elastico-viscous Liquid Between Two Co-axial Cylinders by Artificial Neural Network

U. K. Tripathy^{#1} and S. M. Patel^{*2}

^{#1} Retd. Professor & Head Dept of Mathematics, V.S.S.University, Burla-768017, Sambalpur, India.

^{*2}Lecturer, Department of Mathematics, Sundargarh Engineering School, Sundargarh. 7700073, India

*Corresponding Author: S. M. Patel

Abstract: In this paper an approximate analysis of free convective flow of a non-Newtonian liquid between two co-axial cylinders has been carried out by two techniques. The equation of motion and energy including viscous dissipative terms are a pair of simultaneous non-linear ordinary differential equations. These equations under appropriate boundary conditions have been solved by the fourth order Runge-Kutta method and the back propagation neural networks method. The truncation errors involved in Runge-Kutta method of solution have been determined for one set of values of parameters and have been noted to be $O(10^{-5})$. It has been observed that the elastic parameter has greater influence on the velocity field than on the temperature field. The effect of other parameters P_r (Prandtl number), E (Eckert number) etc. on flow and temperature field. The solution has been compared with the results obtained from the ANN model. This study so far reveals that skin friction, Nusselt number both at outer and inner cylinder can alternatively be modeled using the ANN within a reasonable accuracy. The results obtained from the ANN model are in very good agreement with the numerical results. The designed ANN model can be considered and useful alternative and one of the best techniques for solving non-Newtonian fluid flow problems.

Key words: artificial neural network, back-error propagation, non-Newtonian fluid, skin friction, Nusselt number.

I. INTRODUCTION

The free convective viscous flow between vertical heated plates was investigated by [1], [2],[3],[4],[5]. Likewise [6], [7] have studied the free convective viscous flow through a vertical circular pipe when it is heated or cooled uniformly. The magnetohydrodynamic (MHD) flow of non-Newtonian fluids was examined by [8]. The same problems including the effect of frictional heating and distributed sources or sinks was considered by [9]. In the past years free convective laminar flow of a non-Newtonian liquid has gained substantial importance and has attracted the attention of several researchers. The problem of free convective non-Newtonian flow have studied by [10], [11], [12], [13], [14], [15], [16]. Stochastic solvers based on artificial neural networks has been examined widely by the researchers to solve a variety of linear and non-linear differential equations by [17], [18], [19]. The

solved paper Estimation of MHD boundary layer slip flow over a permeable stretching cylinder in the presence of chemical reaction through numerical and ANN modeling by [20]. The solved paper Estimation of the flow and heat transfer in MHD flow of a power law fluid over a porous plate ANNs by [21]. As described by [21] we have solved our present problem.

This paper has been arranged as follows: Section 2 formulations of the problem. In section 3 solutions by method of iteration and artificial neural network method are presented. Section 4, concluded the achievement of this study.

II. FORMULATION OF THE PROBLEM

The rheological equation of state of the elastic-viscous liquid model considered in this paper by [22] in the following form

$$p_{ij} + \lambda_1 \tilde{p}_{ij} = 2\eta_0 e_{ij} + 4\mu_c e_{i\alpha} e_{\alpha j} \quad (i) \quad \text{where}$$

$$\tilde{p}_{ij} = \frac{\partial p^{ij}}{\partial t} + p^{ij} v^k - p^{ik} v^j_{,k} - p^{kj} v^i_{,k} + p^{ij} v^k_{,k}$$

and μ_c is the cross viscous co-efficient.

The desired equations of motion and energy have been solved by iteration technique, the skin friction and the Nusselt number (Nu) at the boundary of the inner and outer wall of the cylinder is calculated. The same skin friction and the Nusselt number (Nu) has been estimated by an artificial neural network (ANN) scheme. And these two results were compared by tables and figures.

We consider a fully developed laminar free convective flow of an incompressible elastic-viscous fluid contained in the annular space between two co-axial circular cylinders. The cylinders are assumed to be vertical and infinitely long.

We work through cylindrical polar coordinates (r, θ, z) . Let the common axis of the cylinders

coincide with the z-axis and radii of the cylinders be a and b ($a > b$). The velocity field (u, v, w) compatible with the equation of continuity is given by

$$u = 0, v = 0 \text{ and } w = w(r) \tag{2.1}$$

The surviving stress components from equation (i) and (2.1) are given by

$$p^{rr} = \mu_c \left(\frac{dw}{dr}\right)^2 \tag{2.2}$$

$$p^{rz} = \mu \left(\frac{dw}{dr}\right) + \lambda_1 \mu_c \left(\frac{dw}{dr}\right)^3 \tag{2.3}$$

and

$$p^{zz} = (\mu_c + 2\lambda_1\mu) \left(\frac{dw}{dr}\right)^2 + 2\lambda_1^2\mu_c \left(\frac{dw}{dr}\right)^4 \tag{2.4}$$

The dissipation function φ is given by

$$\varphi = \mu \left(\frac{dw}{dr}\right)^2 + \lambda_1 \mu_c \left(\frac{dw}{dr}\right)^4 \tag{2.5}$$

Since the buoyancy force is only due to gravity acting vertically down words, the components of the extraneous force are

$$F_r = 0, F_\theta = 0 \text{ and } F_z = f_z \tag{2.6}$$

Using the Boussine equation approximation the equation of motion can be written as

$$\frac{d^2w}{dr^2} + \frac{1}{r} \frac{dw}{dr} + \frac{\lambda_1\mu_c}{\mu} \left[\frac{d}{dr} \left(\frac{dw}{dr}\right)^3 + \frac{1}{r} \left(\frac{dw}{dr}\right)^3\right] + \frac{\rho\beta f_z}{\mu} \theta' = 0 \tag{2.7}$$

Where β is the volumetric co-efficient of thermal expansion and θ' is the temperature.

The energy equation including viscous dissipative term is given by

$$\frac{d^2\theta'}{dr^2} + \frac{1}{r} \frac{d\theta'}{dr} + \frac{\mu}{k} \left(\frac{dw}{dr}\right)^2 + \frac{\lambda_1\mu_c}{k} \left(\frac{dw}{dr}\right)^4 = 0 \tag{2.8}$$

where k is the thermal conductivity of the fluid. Assuming that the inner cylinder to be moving parallel to itself in the z-direction with constant velocity w and the outer one to be fixed, the boundary conditions for the momentum equation (2.7) are

$$\begin{aligned} r = b : w &= W \\ r = a : w &= 0 \end{aligned} \tag{2.9}$$

Further assuming the temperatures of the inner and outer cylinders to be θ'_b and θ'_a and $\theta'_b > \theta'_a (= 0)$, the boundary conditions to which the energy equation (2.8) is subjected to

$$\begin{aligned} r = b : \theta' &= \theta'_b \\ r = a : \theta' &= 0 \end{aligned} \tag{2.10}$$

We now introduce the following quantities for non-dimensionalizing the above equations.

$$\begin{aligned} h &= a - b, \quad \lambda = \frac{h}{b}, \quad \eta = \frac{r - b}{a - b}, \\ \bar{w} &= \frac{w}{W}, \quad \tau = \frac{\theta'}{\theta'_b}, \quad G = \frac{\rho\beta f_z h^2 \theta'_b}{w\mu}, \end{aligned} \tag{2.11}$$

$$R_c = \frac{\lambda_1\mu_c W^2}{\mu h^2}, \quad E = \frac{w^2}{\theta'_b \theta}, \quad Pr = \frac{\mu_c}{k}$$

where c is the specific heat, θ, R_c, E and Pr respectively denote the Grashof number, elastic number, Eckert number and Prandtl number. Thus the equation of the motion and energy and desired boundary conditions are

$$\frac{d^2\bar{w}}{d\eta^2} + \frac{\lambda}{1 + \lambda\eta} \frac{d\bar{w}}{d\eta} + R_c \left\{ \frac{d}{d\eta} \left(\frac{d\bar{w}}{d\eta}\right)^3 + \frac{\lambda}{1 + \lambda\eta} \left(\frac{d\bar{w}}{d\eta}\right)^3 \right\} + G\tau = 0 \tag{2.12}$$

$$\frac{d^2\tau}{d\eta^2} + \frac{\lambda}{1 + \lambda\eta} \frac{d\tau}{d\eta} + EPr \left\{ \left(\frac{d\bar{w}}{d\eta}\right)^2 + R_c \left(\frac{d\bar{w}}{d\eta}\right)^4 \right\} = 0 \tag{2.13}$$

and

$$\begin{aligned} \eta = 0 : \bar{w} &= 1, \quad \tau = 1 \\ \eta = 1 : \bar{w} &= 0, \quad \tau = 0 \end{aligned} \tag{2.14}$$

III. SOLUTION OF THE GOVERNING EQUATIONS

It is seen that the equation (2.12) and (2.13) are a pair of non-linear equations. We solve this pair of equation under the boundary conditions (2.14) in two different methods viz (i) iteration method and (ii) ANN method.

3.1 Solution by Method of Iteration

Following [23] for solution by iteration we define the sequence of functions $\{\bar{w}_n\}$ and $\{\tau_n\}$ given by

$$\begin{aligned} \bar{w}_n'' + \frac{\lambda}{1 + \lambda\eta} \bar{w}_n' + R_c \left[\frac{d}{d\eta} (\bar{w}_{n-1}')^3 + \frac{\lambda}{1 + \lambda\eta} (\bar{w}_{n-1}')^3 \right] + G\tau_n = 0 \end{aligned} \tag{3.1}$$

$$\begin{aligned} \tau_n'' + \frac{\lambda}{1 + \lambda\eta} \tau_n' + EPr [(\bar{w}_{n-1}')^2 + R_c (\bar{w}_{n-1}')^4] = 0 \end{aligned} \tag{3.2}$$

$$\begin{cases} \bar{w}_n(0) = \tau_n(0) = 1 \\ \bar{w}_n(1) = \tau_n(1) = 0 \end{cases} \quad n = 1, 2, 3, \dots \tag{3.3}$$

and

$$\bar{w}'_{-1} = \bar{w}''_{-1} = 0 \tag{3.4}$$

Primes in the above equations denote differentiation with regard to η .

From equation (3.1) - (3.4) the zeroth order iterate equations are

$$\bar{w}_0'' + \frac{\lambda}{1 + \lambda\eta} \bar{w}_0' + G\tau_0 = 0 \tag{3.5}$$

$$\tau_0'' + \frac{\lambda}{1 + \lambda\eta} \tau_0' = 0 \tag{3.6}$$

And

$$\begin{cases} \bar{w}_0(0) = \tau_0(0) = 1 \\ \bar{w}_0(1) = \tau_0(1) = 0 \end{cases} \tag{3.7}$$

The zeroth order solutions are

$$\tau_0 = 1 - \frac{1}{L} \log(1 + \lambda\eta) \tag{3.8}$$

And

$$\begin{aligned} \bar{w}_0 = \log(1 + \lambda\eta) [A_1(1 + \lambda\eta)^2 + A_2] \\ + A_3(1 + \lambda\eta)^2 + A_4 \end{aligned} \tag{3.9}$$

Where

$$L = \log(1 + \lambda\eta)$$

$$A_1 = \frac{G}{(4L^2)}$$

$$A_2 = -\frac{1}{L} \left[1 + \frac{G}{4\lambda^2} \left\{ 1 - \frac{\lambda(2 + \lambda)}{L} \right\} \right]$$

$$A_3 = -\frac{G}{4\lambda^2} \left(1 - \frac{1}{L} \right)$$

$$A_4 = 1 - A_3$$

We next solve the first order iterative equations which are obtained by setting $n=1$ in equations (3.1) – (3.3). These equations are

$$\begin{aligned} \bar{w}_1'' + \frac{\lambda}{1 + \lambda\eta} \bar{w}_1' + R_c \left[\frac{d}{d\eta} (\bar{w}_0')^3 \right. \\ \left. + \frac{\lambda}{1 + \lambda\eta} (\bar{w}_0')^3 \right] + G\tau_1 = 0 \end{aligned} \tag{3.10}$$

$$\begin{aligned} \tau_1'' + \frac{\lambda}{1 + \lambda\eta} \tau_1' + EP\tau [(\bar{w}_0')^2 + R_c(\bar{w}_0')^4] \\ = 0 \end{aligned} \tag{3.11}$$

and

$$\begin{cases} \bar{w}_1(0) = \tau_1(0) = 1 \\ \bar{w}_1(1) = \tau_1(1) = 0 \end{cases} \quad n = 1, 2, 3, \dots \tag{3.12}$$

Using equations (3.9) in equations (3.10) and (3.11) and solving these equations under the boundary conditions (3.12). We obtain the first order iterates τ_1 , and \bar{w}_1 as in [23].

The solution can be carried to higher order approximation but the algebra involved in this becomes complicated and for this we stop at the first order approximation.

From equation (2.3) and (2.11) the skin friction in the dimensionless form at the inner and outer cylinder can be written as

$$\begin{aligned} \sigma_0 = \left. \frac{h}{\mu\bar{w}} p^{rz} \right]_{\eta=0} \\ = \left[\frac{d\bar{w}}{d\eta} + R_c \left(\frac{d\bar{w}}{d\eta} \right)^2 \right]_{\eta=0} \end{aligned} \tag{3.13}$$

And

$$\begin{aligned} \sigma_1 = \left. \frac{h}{\mu\bar{w}} p^{rz} \right]_{\eta=1} \\ = \left[\frac{d\bar{w}}{d\eta} + R_c \left(\frac{d\bar{w}}{d\eta} \right)^2 \right]_{\eta=1} \end{aligned} \tag{3.14}$$

Now writing $\bar{w} = \bar{w}_1$ in equations (3.13) and (3.14). We obtain the skin frictions σ_0 , σ_1 , and Nusselt numbers Nu_0 , Nu_1 as in [23].

3.2 Artificial Neural Network Method

The artificial neural network (ANN) is a parallel processing architecture consisting of very simple and extremely interconnected processors called neurons organized in layers. Artificial neural network (ANN) is a mathematical model and advanced computing tool that processes information using neuro computing technique. ANN has the capability for machine learning and pattern matching. In an ANN the data or the information is distributed through the network and stored in the form of weighted interconnection. ANN has been shown to be highly flexible modeling tool with the capability of learning the mathematical mapping tool with the capability of learning the mathematical mapping between input and output. ANN is composed of layers of neurons. The input layer of neurons is connected to the output layers of neurons through one or more hidden layers of neurons. ANN is trained with experimental data and tested with other experimental data to reach at an optimum topology and weights.

A back error propagation (BEP) neural network model is considered with one hidden layer with a sigmoid function. During the training process ANN adjusts its weights to minimize the errors between the predicated result and actual output by using Back Propagation algorithm. A schematic diagram of a Back propagation Neural Network (BPNN) with n inputs nodes, r outputs nodes and a single hidden layer of m nodes called processing units is shown in figure 1. Each interconnection between the nodes has a weight associate with it. The input nodes have a transfer function of unity and the

activation function of the hidden and output nodes are sigmoidal $S(.)$ and linear, respectively.

The output of ANN was determined by giving the inputs and computing the output from various nodes activation and interconnection weights. The output was compared to the experimental output and the mean squared error was calculated. The error value was then propagated backwards through the network and changes were made to the weights at each node in each layer. The whole process was repeated, in an iterative fashion, until the overall error value drops below a predetermined threshold.

In the present study, the numerical values obtained for all the parameters were used to train the ANN. The BPNN consists of three phases, namely the training, validation and test phases. The five parameters (λ, G, R_c, E and Pr) determined for the samples used in the study were used as the input nodes and four parameters (Nu_0, Nu_1, σ_0 and σ_1) in these samples were used as the output parameter of the ANN, as shown in figure 1. As there exists no proper rule for setting the exact number of neurons in the hidden layer to avoid overfitting or underfitting of the input parameters and to make the learning phase convergent. The number of nodes in the hidden layer was selected through trial and error method based on the number of epochs needed to train the network. After such iterative procedures it was found that the convergence between the numerical values and predicted values of Nu_0, Nu_1, σ_0 and σ_1 was achieved with the inclusion of one hidden layer with seven neurons. ANN structure has been designed and accomplished using the MATLAB code. A sigmoid function has been used as the activation function of artificial neurons and training has used as the activation function of artificial neurons, and training has been completed using a fixed (2962) number of epochs with a bias of (0.66). The total 27 numerical data set were used to train, validate and test the ANN model for the skin friction coefficient. The 17 data sets were used for the training set, 5 data sets were used for validate and the rest of the data were used for testing the result of the model. The performances of the Nu_0, Nu_1, σ_0 and σ_1 for training, validation and test sets of the proposed ANN model are shown in figure 2(a),(b),(c),(d), figure 3(a),(b),(c),(d), figure 4(a),(b),(c),(d), and figure 5 (a),(b),(c),(d), respectively.

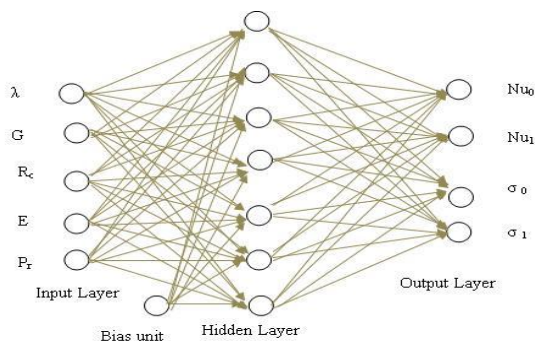


Figure 1. A schematic diagram of a Backpropagation Neural Networks

Following [24] from Tables 1-4 the $y=mx+c$, R^2 , RSME values of the model for all data set were calculated. It is observed that the ANN models were properly trained, as they simulate complicated relationship between the input and output variables. Moreover, the predicted skin friction coefficient, Nusselt number both at outer and inner cylinder values from the ANN model for training, validation and test sets are compared with numerically obtained skin friction coefficient, nusselt number both at outer and inner cylinder values, which are given in figure 2 (a),(b),(c) and (d) to figure 5 (a),(b),(c) and (d) respectively. The results obtained from the ANN model are in very good agreement with the numerical results. This study so far reveals that skin friction, Nusselt number both at outer and inner cylinder can alternatively be modeled using the ANN within a reasonable accuracy. The results obtained from the ANN model are in very good agreement with the numerical results.

IV. CONCLUSION

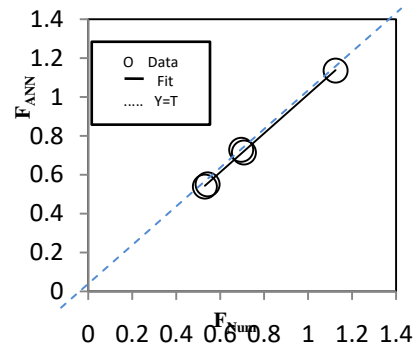
The validity and accuracy of the results by ANN are compared with the available results by Runge-Kutta method and are shown in tables 1–4. It is observed that the above results are found by ANN to be in excellent agreement. The values of skin friction coefficient, Nusselt number and the both at outer and inner cylinder for various values of the involved pertinent parameters are shown in above maintained tables.

Table 1 and 2 gives the values of σ_0 (skin friction at the inner cylinder) and σ_1 (skin friction at the outer cylinder) for different sets of values of the flow parameters. It is observed that σ_0 increases and σ_1 decreases as G, R_c, E and Pr increases. However when λ increases both σ_0 and σ_1 decreases. Table 3 and 4 gives the values of Nusselt number Nu_0 (the rate of heat transfer of inner cylinder) and Nu_1 (the rate of heat transfer of outer cylinder) for various values of the parameters. It is observed that λ and Pr increases both Nu_0 and Nu_1 increases when the parameter R_c and E increases it is seen that Nu_0 increases and Nu_1 decreases. However when G increases both Nu_0 and Nu_1 decreases.

The ANN scheme is also employed for the estimation of σ_0, σ_1, Nu_0 and Nu_1 . The developed ANN scheme is found to be acceptable due to an almost exact accuracy during training, validation and test. These estimated values of ANN are in agreement of 5% difference from the numerically calculated values barring few data. Therefore the designed ANN model can be considered and useful alternative and one of the best techniques for solving non-Newtonian fluid flow problems.

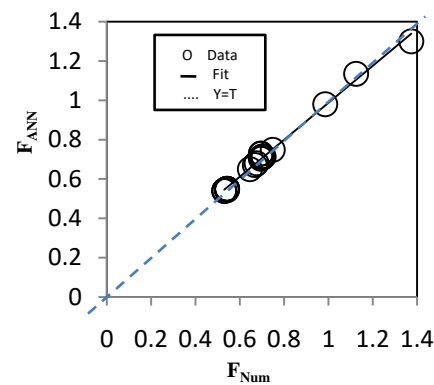
Table 1. Skin friction data of σ_0 for ANN σ_0 and Num σ_0 with error.

Sl. No.	λ	G	Rc	E	Pr	Num σ_0	ANN σ_0	% Error
1	0.8	5	0.00	0.01	1.00	0.53010	0.54231	2.303338993
2	0.8	5	0.01	0.01	1.00	0.53017	0.53928	1.718316766
3	0.8	5	0.05	0.01	1.00	0.53029	0.54011	1.851816930
4	0.8	10	0.00	0.01	1.00	0.54200	0.54298	0.180811808
5	0.8	10	0.01	0.01	1.00	0.54219	0.55011	1.460742544
6	0.8	10	0.05	0.01	1.00	0.54276	0.54999	1.332080478
7	0.8	40	0.00	0.01	1.00	0.54265	0.55019	1.389477564
8	0.8	40	0.01	0.01	1.00	0.54278	0.54972	1.278602749
9	0.8	40	0.05	0.01	1.00	0.54295	0.55001	1.300303895
10	0.2	5	0.00	0.01	1.00	0.69513	0.70925	2.031274726
11	0.2	5	0.01	0.01	1.00	0.69556	0.73001	4.952843752
12	0.2	5	0.05	0.01	1.00	0.69578	0.72812	4.648020926
13	0.2	10	0.00	0.01	1.00	0.70163	0.71018	1.218590995
14	0.2	10	0.01	0.01	1.00	0.70195	0.71329	1.615499679
15	0.2	10	0.05	0.01	1.00	0.70223	0.71516	1.841277074
16	0.2	40	0.00	0.01	1.00	0.70119	0.71008	1.267844664
17	0.2	40	0.01	0.01	1.00	0.70113	0.71025	1.300757349
18	0.2	40	0.05	0.01	1.00	0.70186	0.71294	1.578662411
19	0.8	5	0.01	0.01	0.05	0.64600	0.65018	0.647058824
20	0.8	5	0.01	0.01	0.70	0.66842	0.67124	0.421890428
21	0.8	5	0.01	0.01	1.00	0.69555	0.70296	1.065343972
22	0.8	5	0.01	0.05	0.05	0.67592	0.68012	0.621375311
23	0.8	5	0.01	0.05	0.70	0.70813	0.71396	0.823295158
24	0.8	5	0.01	0.05	1.00	0.74887	0.74821	0.088132787
25	0.8	5	0.01	0.10	0.05	0.98592	0.98012	0.588283025
26	0.8	5	0.01	0.10	0.70	1.12496	1.13528	0.917365951
27	0.8	5	0.01	0.10	1.00	1.37464	1.30010	5.422510621



$y = 1.001x + 0.012, R^2 = 0.997, RSME = 0.01626$

Figure 2(c) Test



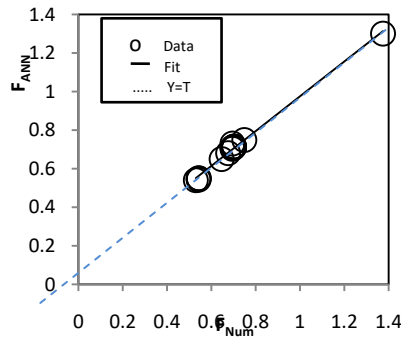
$y = 0.938x + 0.048, R^2 = 0.994, RSME = 0.01877$

Figure 2(d) All

Figure 2 (a), (b),(c)and(d) Graphical representation of σ_0

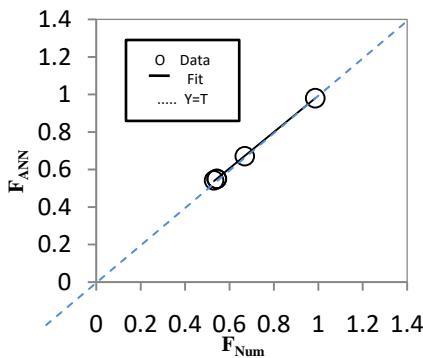
Table 2. Skin friction data of σ_1 for ANN σ_1 and Num σ_1 with error σ_1

Sl. No	λ	G	Rc	E	Pr	Num σ_1	ANN σ_1	% Error
1	0.8	5	0.00	0.01	1.00	-0.45425	-0.45329	0.21133
2	0.8	5	0.01	0.01	1.00	-0.45419	-0.4532	0.21797
3	0.8	5	0.05	0.01	1.00	-0.45318	-0.46128	1.78736
4	0.8	10	0.00	0.01	1.00	-0.47928	-0.46296	3.40510
5	0.8	10	0.01	0.01	1.00	-0.47921	-0.47001	1.91982
6	0.8	10	0.05	0.01	1.00	-0.47781	-0.46925	1.79150
7	0.8	40	0.00	0.01	1.00	-0.47986	-0.48012	0.05418
8	0.8	40	0.01	0.01	1.00	-0.47953	-0.47001	1.98527
9	0.8	40	0.05	0.01	1.00	-0.47886	-0.46992	1.86693
10	0.2	5	0.00	0.01	1.00	-0.36225	-0.37012	2.17253
11	0.2	5	0.01	0.01	1.00	-0.36218	-0.35926	0.80622
12	0.2	5	0.05	0.01	1.00	-0.36017	-0.35958	0.16381
13	0.2	10	0.00	0.01	1.00	-0.39685	-0.39007	1.70845
14	0.2	10	0.01	0.01	1.00	-0.39656	-0.38999	1.65674
15	0.2	10	0.05	0.01	1.00	-0.39617	-0.40003	0.97432
16	0.2	40	0.00	0.01	1.00	-0.39697	-0.38057	4.13129
17	0.2	40	0.01	0.01	1.00	-0.39669	-0.39001	1.68393
18	0.2	40	0.05	0.01	1.00	-0.39625	-0.38826	2.01640
19	0.8	5	0.01	0.01	0.05	-0.36218	-0.35928	0.80070
20	0.8	5	0.01	0.01	0.70	-0.37595	-0.36999	1.58531



$y = 0.902x + 0.072, R^2 = 0.995, RSME = 0.02154$

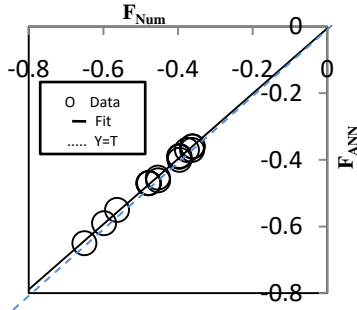
Figure 2(a) Training



$y = 0.966x + 0.026, R^2 = 0.999, RSME = 0.00778$

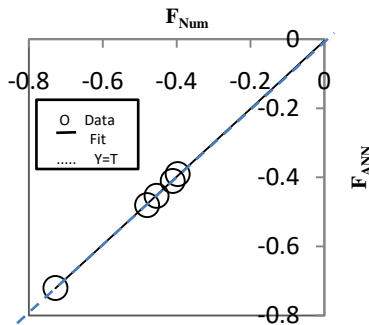
Figure 2(b) Validation

21	0.8	5	0.01	0.01	1.00	-0.41057	-0.40999	0.14126
22	0.8	5	0.01	0.05	0.05	-0.56329	-0.55012	2.33804
23	0.8	5	0.01	0.05	0.70	-0.59827	-0.59007	1.37061
24	0.8	5	0.01	0.05	1.00	-0.68597	-0.67928	0.97526
25	0.8	5	0.01	0.10	0.05	-0.65093	-0.64993	0.15362
26	0.8	5	0.01	0.10	0.70	-0.72815	-0.72008	1.10828
27	0.8	5	0.01	0.10	1.00	-0.8097	-0.79998	1.20044



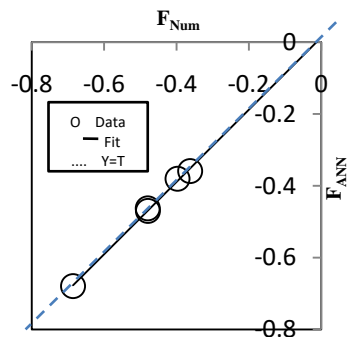
$y = 0.980x - 0.005, R^2 = 0.997, RSME = 0.007372$

Figure 3(a) Training



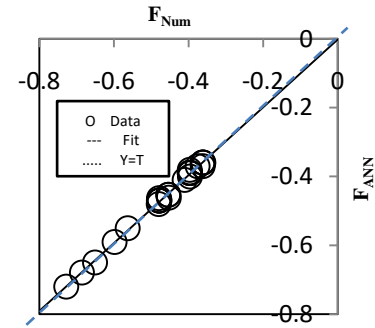
$y = 0.984x - 0.004, R^2 = 0.999, RSME = 0.004741$

Figure 3(b) Validation



$y = 1.006x + 0.013, R^2 = 0.997, RSME = 0.011562$

Figure 3(c) Test



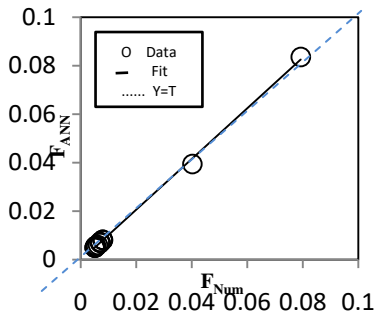
$y = 0.985x - 0.001, R^2 = 0.997, RSME = 0.007946$

Figure 3(d) All

Figure 3 (a), (b), (c) and (d). Graphical representation of σ_1

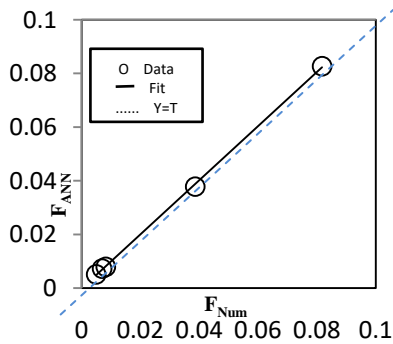
Table 3. Skin friction data of Nu_0 for (Num) Nu_0 and (ANN) Nu_0 with error.

Sl. No.	λ	G	Rc	E	Pr	(Num) Nu_0	(ANN) Nu_0	% Error
1	0.8	5.0	0.01	0.01	0.5	0.00563	0.00576	2.30905
2	0.8	5.0	0.01	0.01	0.7	0.00620	0.00598	3.54838
3	0.8	5.0	0.01	0.01	1.0	0.00798	0.00801	0.37593
4	0.8	5.0	0.01	0.05	0.5	0.03856	0.03782	1.91908
5	0.8	5.0	0.01	0.05	0.7	0.04021	0.03942	1.96468
6	0.8	5.0	0.01	0.05	1.0	0.04336	0.04521	4.26660
7	0.8	5.0	0.01	0.10	0.5	0.07925	0.08362	5.51419
8	0.8	5.0	0.01	0.10	0.7	0.08173	0.08269	1.17459
9	0.8	5.0	0.01	0.10	1.0	0.08927	0.09412	5.43295
10	0.2	5.0	0.00	0.01	1.0	0.00530	0.00499	5.84905
11	0.2	5.0	0.01	0.01	1.0	0.00539	0.00542	0.55658
12	0.2	5.0	0.05	0.01	1.0	0.00547	0.00572	4.57038
13	0.2	10.0	0.00	0.01	1.0	0.00526	0.00534	1.52091
14	0.2	10.0	0.01	0.01	1.0	0.00531	0.00557	4.89642
15	0.2	10.0	0.05	0.01	1.0	0.00538	0.00576	7.06319
16	0.2	40.0	0.00	0.01	1.0	0.00489	0.00512	4.70347
17	0.2	40.0	0.01	0.01	1.0	0.00496	0.00492	0.80645
18	0.2	40.0	0.05	0.01	1.0	0.00508	0.00488	3.93700
19	0.8	5.0	0.00	0.01	1.0	0.00785	0.00816	3.94904
20	0.8	5.0	0.01	0.01	1.0	0.00798	0.00812	1.75438
21	0.8	5.0	0.05	0.01	1.0	0.00816	0.00795	2.57352
22	0.8	10.0	0.00	0.01	1.0	0.00701	0.00728	3.85164
23	0.8	10.0	0.01	0.01	1.0	0.00709	0.00697	1.69252
24	0.8	10.0	0.05	0.01	1.0	0.00723	0.00698	3.45781
25	0.8	40.0	0.00	0.01	1.0	0.00686	0.00714	4.08163
26	0.8	40.0	0.01	0.01	1.0	0.00692	0.00729	5.34682
27	0.8	40.0	0.05	0.01	1.0	0.00705	0.00687	2.55319



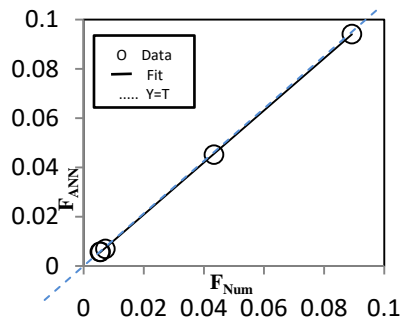
$y = 1.045x - 0.000, R^2 = 0.998, RSME = 0.001094$

Figure 4 (a) Training



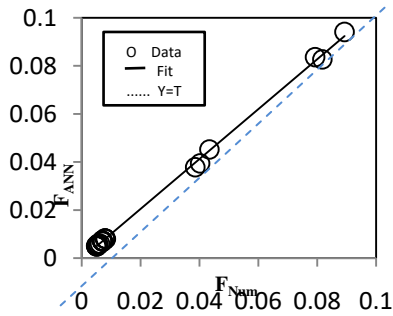
$y = 1.008x - 0.000, R^2 = 0.999, RSME = 0.000583$

Figure 4 (b) Validation



$y = 1.056x - 0.000, R^2 = 0.999, RSME = 0.002331$

Figure 4 (c) Test



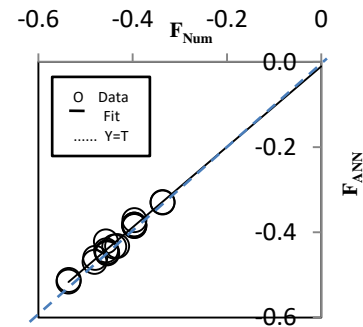
$y = 1.038x - 0.000, R^2 = 0.999, RSME = 0.001350$

Figure 4 (d) All

Figure 4 (a), (b), (c) and (d). Graphical representation of Nu_0

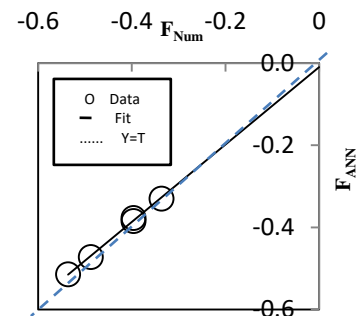
Table 4. Skin friction data of Nu_1 for (Num) Nu_1 and (ANN) Nu_1 with error.

Sl. No.	λ	G	Rc	E	Pr	(Num) Nu_1	(ANN) Nu_1	% Error
1	0.8	5.0	0.01	0.01	0.5	-0.33657	-0.33001	1.94907
2	0.8	5.0	0.01	0.01	0.7	-0.33655	-0.32995	1.96107
3	0.8	5.0	0.01	0.01	1.0	-0.33652	-0.32897	2.24355
4	0.8	5.0	0.01	0.05	0.5	-0.43921	-0.43321	1.36608
5	0.8	5.0	0.01	0.05	0.7	-0.43385	-0.43106	0.64307
6	0.8	5.0	0.01	0.05	1.0	-0.43301	-0.43216	0.19630
7	0.8	5.0	0.01	0.10	0.5	-0.53623	-0.51567	3.83417
8	0.8	5.0	0.01	0.10	0.7	-0.53598	-0.51428	4.04865
9	0.8	5.0	0.01	0.10	1.0	-0.53561	-0.51172	4.46033
10	0.2	5.0	0.00	0.01	1.0	-0.45415	-0.45000	0.91553
11	0.2	5.0	0.01	0.01	1.0	-0.45419	-0.44926	1.08544
12	0.2	5.0	0.05	0.01	1.0	-0.45431	-0.44632	1.75846
13	0.2	10.0	0.00	0.01	1.0	-0.45664	-0.44213	3.17686
14	0.2	10.0	0.01	0.01	1.0	-0.45673	-0.42137	7.74217
15	0.2	10.0	0.05	0.01	1.0	-0.45708	-0.42119	7.85179
16	0.2	40.0	0.00	0.01	1.0	-0.47939	-0.46013	4.01818
17	0.2	40.0	0.01	0.01	1.0	-0.48101	-0.46938	2.41904
18	0.2	40.0	0.05	0.01	1.0	-0.48750	-0.47210	3.16016
19	0.8	5.0	0.00	0.01	1.0	-0.39660	-0.38221	3.62906
20	0.8	5.0	0.01	0.01	1.0	-0.39660	-0.38167	3.76344
21	0.8	5.0	0.05	0.01	1.0	-0.39661	-0.38170	3.75935
22	0.8	10.0	0.00	0.01	1.0	-0.39656	-0.38516	2.87568
23	0.8	10.0	0.01	0.01	1.0	-0.39656	-0.38429	3.09530
24	0.8	10.0	0.05	0.01	1.0	-0.39657	-0.38431	3.09143
25	0.8	40.0	0.00	0.01	1.0	-0.39639	-0.37121	6.35105
26	0.8	40.0	0.01	0.01	1.0	-0.39639	-0.38010	4.10931
27	0.8	40.0	0.05	0.01	1.0	-0.39639	-0.37692	4.91301



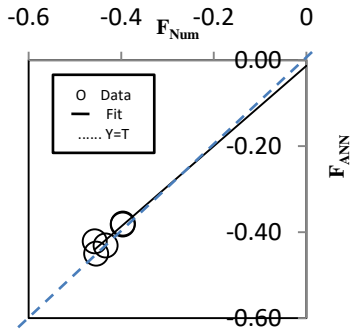
$y = 0.943x - 0.010, R^2 = 0.978, RSME = 0.016351$

Figure 5 (a) Training

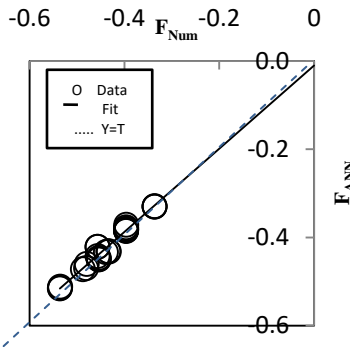


$y = 0.942x - 0.009, R^2 = 0.997, RSME = 0.016007$

Figure 5 (b) Validation



$y = 0.935x - 0.013, R^2 = 0.818, RSME = 0.018897$
Figure 5 (c) Test



$y = 0.943x - 0.010, R^2 = 0.975, RSME = 0.016790$
Figure 5 (d) All

Figure 5 (a), (b), (c) and (d). Graphical representation of Nu_1

REFERENCES

[1] Ostrach, S., (1952). NACA, TN, 2863.
 [2] Ostrach, S., (1954). Jbid, 3141.
 [3] Ostrach, S., (1955)(a). Sondrdruck aus, 50, Jhara, Grenz, Viewg, Braun, 226.

[4] Ostrach, S., (1955)(b). NACA, TN, 3458.
 [5] Ostrach, S., (1957). INTUM, Boundary Layer Research Freiburg, 185.
 [6] Morton, B.R., (1960). J. Fluid. Mech. 8, 227.
 [7] Tau, L.N., (1960). Appl. Sci. Res. A(9), 357.
 [8] Sarpakaya, T., (1961). Flow of non-Newtonian fluids in a magnetic field, AICHE Journal, 7(2): 324-328.
 [9] Nanda, R.S. and Sharma, V.P., (1962). Appl. Sc. Res. A(11) 279.
 [10] Achivos, A., (1960). A. J. Ch. E. Journal, 6,584.
 [11] Mishra, S.P., (1965). Proc. Ind. Acad. Sci., 61(4A), 219.
 [12] Hansen, A.J. and Na,T.Y., (1966). Int. J. Heat and Mass Transfer, 9, 261.
 [13] Kabeir, V.G. and Pai, D.C.T., (1968). A.R.C.11, 855.
 [14] Emery, A.F., Chi, H.W. and Dale, J.D., (1971).Trans, ASME 93(2), 164.
 [15] Mishra, S. P. and Acharya, B.P., (1972). Ind. J. Phys., 46,469.
 [16] Acharya, B.P., (1975). Prc. Ind. Acad. Sci, 3, 99.
 [17] McFal, K.S., (2013). Automated design parameter section for neural networks solving coupled partial differential equations, Journal of the Franklin Institute-Engineering and Applied Mathematics, 350(2): 300-317.
 [18] Tsoulos, I.J., Gavrilis, D. and Glavas, E., (2009). Solving differential equations with constructed neural networks, Neurocomputing, 72 (10-12): 2385-2391.
 [19] Choi, B. and Lee, J.H., (2009). Comparison of generalization ability on solving differential equations using backpropagation and reformulated radial basis function networks, Neurocomputing, 73(1-3): 115-118.
 [20] Reddy, P.B.A. and Das, R., (2016). Estimation of MHD boundary layer slip flow over a permeable stretching cylinder in the presence of chemical reaction through numerical and ANN modeling, Engineering Science and Technology, an International Journal, doi: 10.
 [21] Shahri, M.F. and Nezhad, A.F., (2014). Estimation of the flow and heat transfer in MHD flow of a power law fluid over a porous plate ANNs, Middle East J. Sci. Res. 22(9) 1422-1429
 [22] Noll, W., (1955). J. Rat. Mech. Anal., 4, 3.
 [23] Tripathy, U.K., (1980). Ph.D. Thesis, Utkal University, Bhubaneswar.
 [24] Tripathy, U.K. and Patel S.M., (2017). On Heat Transfer in case of a Viscous Flow over a Plane Wall with Periodic Suction by Artificial Neural Network. IJMTT-Vol. 44 number 2 April.